



Using radiomics-based modelling to predict individual progression from mild cognitive impairment to Alzheimer's disease

Jiehui Jiang¹ · Min Wang¹ · Ian Alberts² · Xiaoming Sun¹ · Taoran Li³ · Axel Rominger² · Chuantao Zuo^{4,5} · Ying Han^{3,6,7,8} · Kuangyu Shi^{2,9} · for the Alzheimer's Disease Neuroimaging Initiative

Received: 2 August 2021 / Accepted: 11 January 2022

© The Author(s), under exclusive licence to Springer-Verlag GmbH Germany, part of Springer Nature 2022

Abstract

Background Predicting the risk of disease progression from mild cognitive impairment (MCI) to Alzheimer's disease (AD) has important clinical significance. This study aimed to provide a personalized MCI-to-AD conversion prediction via radiomics-based predictive modelling (RPM) with multicenter 18F-fluorodeoxyglucose positron emission tomography (FDG PET) data.

Method FDG PET and neuropsychological data of 884 subjects were collected from Huashan Hospital, Xuanwu Hospital, and from the Alzheimer's Disease Neuroimaging Initiative (ADNI) database. First, 34,400 radiomic features were extracted from the 80 regions of interest (ROIs) for all PET images. These features were then concatenated for feature selection, and an RPM model was constructed and validated on the ADNI dataset. In addition, we used clinical data and the routine semi-quantification index (standard uptake value ratio, SUVR) to establish clinical and SUVR Cox models for further comparison. FDG images from local hospitals were used to explore RPM performance in a separate cohort of individuals with healthy controls and different cognitive levels (a complete AD continuum). Finally, correlation analysis was conducted between the radiomic biomarkers and neuropsychological assessments.

Results The experimental results showed that the predictive performance of the RPM Cox model was better than that of other Cox models. In the validation dataset, Harrell's consistency coefficient of the RPM model was 0.703 ± 0.002 , while those of the clinical and SUVR models were 0.632 ± 0.006 and 0.683 ± 0.009 , respectively. Moreover, most crucial imaging biomarkers were significantly different at different cognitive stages and significantly correlated with cognitive disease severity.

Conclusion The preliminary results demonstrated that the developed RPM approach has the potential to monitor progression in high-risk populations with AD.

Keywords Radiomics-based predictive model · Alzheimer's disease · Mild cognitive impairment · Radiomics · Cox model

This article is part of the Topical Collection on Advanced Image Analyses (Radiomics and Artificial Intelligence)

✉ Jiehui Jiang
jjiangjiehui@shu.edu.cn

✉ Chuantao Zuo
zuochuantao@fudan.edu.cn

✉ Ying Han
hanying@xwh.ccmu.edu.cn

¹ Institute of Biomedical Engineering, School of Life Science, Shanghai University, Shanghai, China

² Department of Nuclear Medicine, University Hospital Bern, Bern, Switzerland

³ Department of Neurology, Xuanwu Hospital of Capital Medical University, Beijing, China

⁴ PET Center, Huashan Hospital, Fudan University, Shanghai, China

⁵ Human Phenome Institute, Fudan University, Shanghai, China

⁶ Center of Alzheimer's Disease, Beijing Institute for Brain Disorders, Beijing, China

⁷ School of Biomedical Engineering, Hainan University, Haikou, China

⁸ National Clinical Research Center for Geriatric Disorders, Beijing, China

⁹ Department of Informatics, Technische Universität München, Munich, Germany

Introduction

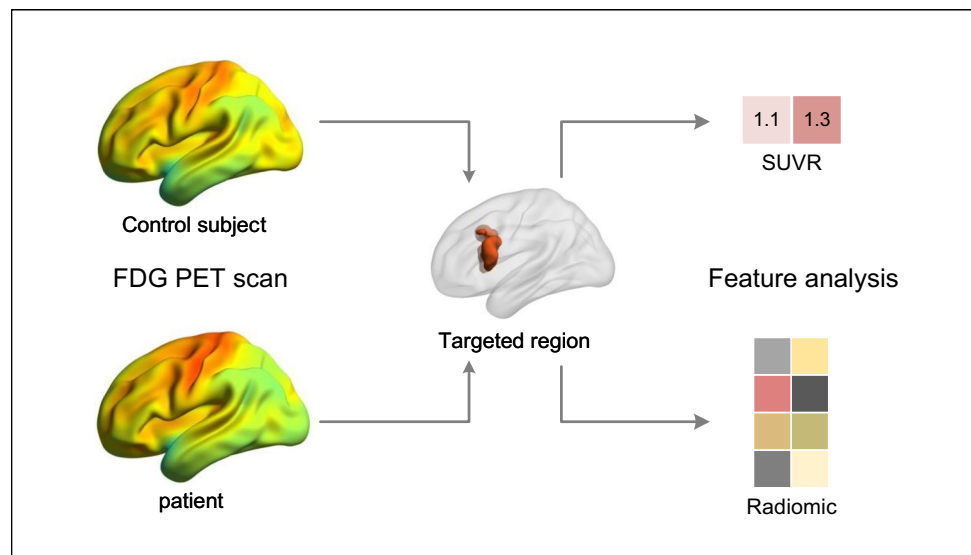
Alzheimer's disease (AD) is the most common neurodegenerative disease and is the leading cause of death for which no disease-modifying therapy is currently available [1, 2]. At present, it has been recognized as a distinct entity and is defined pathologically by the presence of a specific neuropathological profile, i.e., extracellular deposition of β -amyloid ($A\beta$) and Tau, while cognitive impairment is evaluated externally [3, 4]. Meanwhile, cognition is considered a continuum, in which mild cognitive impairment (MCI) refers to individuals who have objective evidence of impaired cognition but preserved independent function and is undisputedly a high-risk factor for AD [5]. The reported annual rate of MCI conversion to AD-dementia is approximately 10%; however, more than 60% of MCI cases likely will not progress, even after 10 years [6–9]. Therefore, clarifying which patients with MCI will develop dementia is of great significance for enriching clinical trials and carrying out prevention strategies for target individuals.

Previous studies have verified that the pathological deposition of $A\beta$ and/or Tau accelerates the progression of MCI, and both biomarkers robustly predict cognitive decline [10]. Nevertheless, their detection results may vary by the use of different ligands, analysis methods, or cut-off values [11–13]. In addition, the invasiveness of lumbar puncture, and the low popularity of amyloid-positron emission tomography (PET) and tau-PET scans further limit their application. Comparatively, [^{18}F] fluoro-2-deoxyglucose (^{18}F -FDG) PET imaging has been widely used in the clinical evaluation of neurodegeneration [14]. Some FDG PET imaging studies, including ours, have obtained

plausible results with high accuracy using principal component analysis or statistical parametric mapping analysis or deep belief network analysis [15–17], suggesting the necessity and potential of glucose metabolism. Furthermore, the standard uptake value ratio (SUVR), the most popular quantification surrogate to present the regional glucose activity, may be very helpful for clinical diagnostic. Previous studies have suggested that applying SUVR as a predictive index to perform an MCI conversion model is feasible [18–20], however, while integral to its role as a predictive biomarker, may require the sacrifice of complete information needed to delineate underlying regional metabolic activity. Therefore, developing advanced biomarkers and predictive models to disclose more metabolic information and further improve its predictive ability remains a significant challenge for MCI-to-AD conversion prediction.

Radiomics aims to extract the high-throughput mining of quantitative image features from specific imaging and to establish relevant statistical models that could improve clinical diagnostic, prognostic, and predictive accuracy; this approach is gaining importance in brain disease research [21, 22]. Quantitative radiomic features (such as intensity, shape, texture, and wavelet) disclose the information on neural activity as well as abnormal regional metabolism that is distinct and complementary to other semiquantitative measurements, such as SUVR. For example, radiomic features, as high dimensional features, represent spatial change rate levels of voxel intensity in the brain (Fig. 1), and may contain unique information about changes at the microscopic level, while SUVR offers only two regional quantitative values. Recently, we showed that the radiomic features extracted from FDG-PET images contribute to the diagnosis of neurodegenerative diseases including AD and Parkinson's disease

Fig. 1 The representative characteristics of routine semi-quantification method (SUVR) and radiomics method. For the targeted region, the radiomics discloses the sensitive and complete information about underlying pathophysiological metabolism, while SUVR method only offers the rough metabolic intensity description



[23–25]. Thus, radiomics-derived features based on FDG PET images, when combined with clinical information and correlated with outcome results, can advance the development of accurate robust predictive models.

Thus, the primary objectives of this study were to (a) establish a radiomics-based prediction model (RPM) of MCI conversion using FDG-PET imaging, (b) investigate the robustness using multicenter cohorts, and (c) explore its performance in a separate cohort including individuals with different cognitive levels (a complete AD continuum). We hypothesized that imaging biomarkers derived from the RPM model may have the potential to predict individual progression risk in MCI patients.

Materials and methods

Subjects

The total sample for the subsequent analysis consisted of FDG PET images from 884 subjects from three different cohorts (Alzheimer Disease Neuroimaging Initiative (ADNI), Huashan Hospital, and Xuanwu Hospital). For construction of the RPM model, a total of 355 patients with either stable MCI (sMCI, $n = 187$) or progressive MCI (pMCI, $n = 168$) and 94 healthy control (HC) subjects were recruited from ADNI-1, ADNI-2, and ADNI-3. Among them, each HC subject had twice longitudinal follow-up (time interval: 2.0 ± 0.05 years) images. We used twice HC images to perform radiomic feature selection and characterize the feature's stability. To evaluate the RPM model's predictive ability, we also collected cohort II from the ADNI-Go database as an independent test dataset, which included 81 sMCI and 39 pMCI patients. Furthermore, to explore the performance of distinct features in the overall AD continuum, 138 HC subjects and a total of 177 patients with either subjective cognitive decline (SCD, $n = 76$), MCI ($n = 41$), or AD ($n = 60$) were collected from local hospitals (Xuanwu Hospital: Sino Longitudinal Study on Cognitive Decline project (SILCODE) project and Huashan Hospital) as cohort III. All subjects underwent FDG PET scans, T1-MPRAGE structural MRI scans, and demographic data. Part of subjects also underwent AV45 amyloid-PET scans. Detailed inclusion information related to subject consent in ADNI could be obtained at <http://adni.loni.usc.edu>. The inclusion criteria of MCI patients enrolled from ADNI database have been reported previously [17] and were as follows: (1) all patients with sMCI and pMCI underwent FDG PET scans and clinical diagnoses at the baseline visit and were followed up for at least 3 years; (2) sMCI patients who had not converted to AD at follow-up and pMCI patients who had converted to AD within the follow-up interval; and (3) participants with a bidirectional change in diagnosis (MCI

to AD, and back to MCI) within the follow-up period were excluded. The inclusion criteria of cohort III have also been reported previously [26]. The entry criteria for healthy individuals have been described previously [27]. The diagnosis of dementia was based on the guidelines of the NIA-AA workgroups [28]; SCD was defined by the research criteria for pre-MCI (SCD) proposed by Jessen et al. in 2014 [29], and MCI was based on neuropsychological methods [30].

For cohort I, the randomized cross validation method was used to randomly partition into a 70% training dataset and a 30% internal test dataset multiple times (100 times). Cohort II was regarded as an independent external test dataset. The amyloid status of ADNI was determined by the global AV45 amyloid-PET SUVR normalized to the whole cerebellum using a pre-established FreeSurfer-based protocol [31]. The amyloid status of individuals in cohort III was determined by the same global AV45 amyloid SUVR. The amyloid level for each subject was confirmed by two senior radiologists who were blinded to any clinical information and made positive or negative judgment. This study was approved by institutional review boards of ADNI, Huashan, and Xuanwu Hospital, and written informed consent was obtained from all participants or authorized representatives.

Acquisition protocol and preprocessing

All subjects in this study were scanned by FDG PET and structural T1 MRI imaging. Detailed information on the data acquisition of ADNI can be found on the website (<http://adni.loni.usc.edu/>). MRI data from Huashan Hospital were acquired with General Electric 3 T MR750 scanner. The subjects in Huashan Hospital underwent FDG PET scanning with Siemens Biograph 64 HD PET/CT. After intravenous injection of 185 MBq FDG, subjects underwent a PET scan after resting for 45 min. MRI and FDG data from Xuanwu Hospital were acquired using General Electric 3 T TOF PET/MR scanner. Approximately 40 min after intravenous injection of 3.7 MB/kg of ^{18}F -FDG, a 35-min dynamic scan was performed. The detailed acquisition protocol has been reported previously [26, 27, 32].

Data preprocessing was performed by using Statistical Parametric Mapping 12 (SPM12, the Wellcome Department of Neurology, London U.K.) implemented in MATLAB 2016b (Mathworks Inc.). First, the original FDG PET image for each subject was registered with the corresponding structural MRI image. Then, MRI images were segmented into gray matter (GM), white matter (WM), and cerebrospinal fluid (CSF) tissue probability maps using the unified segmentation method. The registered PET image was spatially normalized to the MNI space using the transformation parameters. Finally, the normalized PET images were smoothed using an isotropic Gaussian kernel of 8 mm to

increase signal-to-noise ratios. Notably, all FDG PET images underwent count normalization using global cortical uptake.

Radiomics-based predictive modelling analysis

In this study, the RPM method was implemented to develop predictive models of brain-behavior relationships from glucose metabolic data. The RPM method included the following steps: (1) radiomics feature extraction, (2) radiomics feature summarization, and (3) model construction and assessment.

Radiomics feature extraction

To obtain more detailed features, 80 cortical regions from the automated anatomical labelling (AAL) atlas were used as regions of interest (ROIs). We extracted 430 radiomics features from each ROI for FDG PET data. In brief, the most basic features in each ROIs include two parts: first-order intensity features ($n=3$) and texture features ($n=40$). We extracted features under the combination of different wavelet filter weights (5 levels) and quantization of gray levels (2 levels), and the total number of features per ROI was 430 ($(3+40) \times 5 \times 2 = 430$). The details of these features provided in [supplementary](#).

Radiomics feature summarization

The tenfold cross-validation and Z-normalization strategies were implemented in cohort I. To reduce the dimension of features and solve the overfitting problem, three feature selection steps were performed separately for the training data in cohort I: (1) feature stability analysis: stable features with Cronbach's alpha coefficient greater than 0.75 were selected based on longitudinal HC data in cohort I; (2) statistical test: t test and rank sum t test with family-wise error option multiple correction were used to identify the features with significant differences ($P < 0.05$); and (3) least absolute shrinkage and selection operator (LASSO). As a result, radiomic features after the feature summarization steps were considered as the conserved features for the future prediction model.

Model construction and assessment

The proportional hazards model (Cox) model was constructed as the prediction model. The Cox model is a method for investigating the effect of several variables (predictive features) upon the time (conversion time or follow-up interval). Therefore, the outcome of the Cox model in this study was whether MCI subjects converted to AD. The time of outcome appearance was the interval between the baseline time and the endpoint. The Harrell's concordance index (C-index)

was used to evaluate risk models in survival analysis (MCI to AD) [17]. Tenfold cross-validation was used to evaluate the prediction performance. In addition, forwards stepwise selection was employed to choose the optimal feature subset (stopping rule: lowest Akaike information criterion, AIC) in the Cox construction. The Cox model was used in the test dataset to calculate the prognostic index (PI) for each subject. PI was a linear combination of the selected feature and its coefficient. The Kaplan–Meier survival curves analysis based on ranked PI value was employed to examine the differences of MCI conversion rate. A clinical Cox model was also constructed using available clinical variables (age, sex, education, and Mini-Mental State Examination-MMSE) to compare the predictive performance with the RPM method.

To further evaluate the predictive ability, we also compared the conventional regional model, SUVR, with our proposed RPM model. Based on abnormal metabolic regions derived from the SPM test [20], we predefined 6 merged ROIs ([Supplementary Table](#)) and calculated SUVR values in these 6 ROIs as predictive indexes to construct SUVR Cox model. Cohort II data was used for external validation of the predictive model derived from the RPM method [33].

Validation of crucial features

To further explore the relationship between conserved radiomic features and neuropsychiatric assessments at different cognitive stages, correlation coefficients were calculated between the features and neuropsychological assessments (MMSE scores) in the AD continuum (SCD, MCI, and AD subjects) from cohort III. Differences in the crucial features of the HC group and the whole AD continuum were also evaluated to check whether the value distribution of the conserved radiomic features had good consistency in the whole AD spectrum.

Statistical analysis

Subject characteristics were compared between groups using chi-squared tests for categorical variables (sex) and two-sample t tests (cohorts I and II) and ANOVAs (cohort III) for numeric variables (age, education, MMSE, amyloid level, and conversion time). The feature differences of cohort III across groups were statistically analyzed using ANOVA with Dunnett's multiple comparison test. The correlation analyses were repeated using a general linear model controlled for covariates (i.e., age, education, sex), to ensure that the association between radiomic features and MMSE was not driven by these covariates. P values were 2-tailed, and $P < 0.05$ was considered statistically significant. All statistical tests were performed using SPSS 24.0. Cox models were constructed in R (<http://www.R-project.org/>) employing the “glmnet” and “survival” packages [34–36].

Results

Subjects

Table 1 shows the demographic information of the participants from each cohort. There was a higher amyloid level in the pMCI group both cohort I and cohort II ($P < 0.001$), but there was no significant difference in the amyloid level between HC and SCD ($P = 0.49$, Dunnett's correction). Patients with MCI had higher amyloid level than HCs and SCD patients ($P < 0.001$, Dunnett's correction). Cognitive disease severity (MMSE) was significantly different in sMCI compared to pMCI (all $P < 0.001$), in AD compared to HC ($P < 0.001$), and in MCI compared to HC ($P < 0.001$). Measures of MMSE were not significantly different between SCD and HCs ($P = 0.21$).

Conserved features in Cox model

Radiomics analysis was used to extract 34,400 features from PET images of each subject. In the tenfold cross-validation with 100 iterations, we chose the optimal feature subset that was included in the RPM model using a forward stepwise selection approach. This resulted in 11 conserved features in the Cox model (C-index: 0.859; AIC: 1550.2). As shown in Table 2, the conserved features mainly came from the

texture features of the hippocampus, cingulate cortex, parahippocampal gyrus, precuneus, and other frontal regions.

PET model radiomics analysis predicts the progression MCI to AD

Three prediction models were constructed, including the clinical model, SUVR model, and RPM model. This study evaluated the model's prediction performance and identified the conserved features associated with MCI conversion in each model. The average C-index with 100 iterations was used to assess the predictive performance. As summarized in Table 3, there was a superior predictive performance in the RPM model (C-index of train and validation datasets: 0.838 and 0.703), while there was moderate performance in the SUVR model (C-index: 0.788 and 0.683) and lower performance in the clinical model (C-index: 0.692 and 0.632). Figure 2 demonstrates the characteristics of the conserved features found in the RPM model and that of the composite quantification values in the SUVR model and the related Kaplan–Meier survival curves. In the RPM model, zone percentage of left hippocampus showed the strongest predictive power (hazard ratio, HR: 1.465, 95% confidence interval, 95% CI: 1.236–1.737, $P < 0.001$). For cohort II, the Kaplan–Meier survival curves demonstrated good separation of groups with high and low risks of conversion to AD. The best MCI conversion stratification was reached with

Table 1 The clinical characteristics of all cohorts

Group		Sex (M/F)	Age (years)	Education (year)	MMSE	Amyloid β level	Conversion time (months)	
Cohort I	sMCI ($n = 187$)	109/78	72.1 \pm 7.5	16.0 \pm 2.6	28.0 \pm 1.6	1.16 \pm 0.20	0	
	pMCI ($n = 168$)	95/73	74.0 \pm 7.1	16.0 \pm 2.6	26.5 \pm 2.2	1.40 \pm 0.22	14.1 \pm 8.9	
	<i>P</i> value	0.74 ^a	0.018 ^b	0.91 ^b	<0.001 ^b	<0.001 ^b	<0.001	
	HC ($n = 94$)	HC 1	48/46	72.8 \pm 5.9	16.9 \pm 2.4	29.2 \pm 1.2	/	/
		HC 2	48/46	74.8 \pm 5.9	16.9 \pm 2.4	29.1 \pm 1.2	/	/
	<i>P</i> value	1 ^a	<0.001 ^c	1 ^c	0.57 ^c	/	/	
Cohort II	sMCI ($n = 81$)	44/37	72.2 \pm 7.8	15.6 \pm 2.8	28.2 \pm 1.4	1.16 \pm 0.18	0	
	pMCI ($n = 39$)	21/18	72.1 \pm 6.9	16.3 \pm 2.7	26.7 \pm 1.9	1.37 \pm 0.19	16.4 \pm 7.3	
	<i>P</i> value	0.96 ^a	0.68 ^b	0.35 ^b	<0.001 ^b	<0.001 ^b	<0.001	
Cohort III	HC ($n = 138$)	67/71	58.9 \pm 10.5	13.1 \pm 3.1	29.1 \pm 1.2	1.16 \pm 0.07	/	
	SCD ($n = 76$)	12/64	66.1 \pm 5.1	12.9 \pm 2.8	28.9 \pm 0.9	1.15 \pm 0.08	/	
	MCI ($n = 41$)	20/21	66.5 \pm 7.4	12.6 \pm 3.6	24.0 \pm 5.4	1.28 \pm 0.14	/	
	AD ($n = 60$)	23/37	61.7 \pm 10.3	10.1 \pm 2.3	19.3 \pm 7.2	/	/	
	<i>P</i> value	<0.001 ^a	<0.001 ^d	<0.001 ^d	<0.001 ^d	<0.001	/	

^aChi-squared tests; ^btwo samples *t* test; ^cpaired samples *t* test; ^dANOVA test. HC, healthy control; SCD, subjective cognitive decline; MCI, mild cognitive impairment; AD, Alzheimer's disease; sMCI, stable mild cognitive impairment; pMCI, progressive mild cognitive impairment; MMSE, mini-mental state examination

Table 2 Conserved features in the radiomics-based predictive model

Label	Feature	Feature's name	Gray-level	Wavelet filter weights	Texture matrices	Location	Anatomical classification
1	GLV	Gray-level variance	32	3/2	Global features	Left hippocampus	Temporal
2	Correlation	Correlation	64	3/2	Gray-level cooccurrence matrix	Right precuneus	Parietal
3	LGZE	Low gray-level zone emphasis	32	3/2	Gray-level size zone matrix	Left median cingulate	Frontal
4	SZHGE	Small zone high-gray-level emphasis	32	2	Gray-level size zone matrix	Right supramarginal gyrus	Parietal
5	Busyness	Busyness	64	1	Neighborhood gray-tone difference matrix	Left parahippocampal gyrus	Temporal
6	LZLGE	Large zone low gray-level emphasis	32	3/2	Gray-level size zone matrix	Left median cingulate	Frontal
7	ZSV	Zone-size variance	32	2	Gray-level size zone matrix	Left precuneus	Parietal
8	Energy	Energy	64	2	Gray-level cooccurrence matrix	Right cuneus	Parietal
9	Correlation	Correlation	64	1	Gray-level cooccurrence matrix	Right precuneus	Parietal
10	ZP	Zone percentage	32	1	Gray-level size zone matrix	Left hippocampus	Temporal
11	SRLGE	Small zone high-gray-level emphasis	32	2/3	Gray-level run-length matrix	Left superior frontal gyrus	Frontal

Table 3 The prediction performance of each model

Model	Train dataset of cohort I		Test dataset of cohort I		Cohort II	
	C index	AIC	C index	AIC	C index	AIC
Clinical	0.692 ± 0.004	1607.2	0.684 ± 0.006	1622.1	0.632 ± 0.006	1640.1
SUVR	0.788 ± 0.010	1581.3	0.720 ± 0.010	1597.8	0.683 ± 0.009	1615.4
Radiomics	0.838 ± 0.002	1550.2	0.745 ± 0.006	1577.3	0.703 ± 0.002	1598.7

C index, Harrell's concordance index; *AIC*, Akaike information criterion

the prognostic index resulting from the RPM model (RPM model, $P < 0.001$; SUVR model, $P = 0.006$).

Validation of crucial features

As shown in Fig. 3, of 11 conserved radiomic features, five showed significant correlations with the MMSE scores in the AD continuum (SCD, MCI, and AD) of cohort III ($P < 0.05$), including GLV of left hippocampus, LGZE of left median cingulate, ZP of left hippocampus, correlation of right precuneus, and energy of left cuneus. As a result, ZP of left hippocampus had strongest positive relationship ($r = 0.59$, 95% CI: 0.48 ~ 0.68; $P < 0.001$) while the energy of left cuneus had strongest negative relationship ($r = -0.47$, 95% CI: -0.57 ~ -0.35; $P < 0.001$).

We explored differences in these five crucial features in the healthy controls and AD continuum in cohort III. Figure 4 demonstrates examples of feature distributions

at different cognitive stages. The results showed that these features were significantly different (all $P < 0.001$, ANOVA test). In addition, the results showed that all 5 features were significantly different between HC and AD groups (all $P < 0.001$, Dunnett's correction), but no differences were found between SCD and HC groups (all $P > 0.05$, Dunnett's correction).

Discussion

In this study, we proposed a workflow for radiomics-based predictive modelling analysis using FDG PET images. This workflow extracted a large number of quantitative features from PET images and identified crucial biomarkers. Based upon these biomarkers, we built and evaluated Cox regression models to predict the conversion outcome results of MCI patients. Notably, as a multicenter study, we also

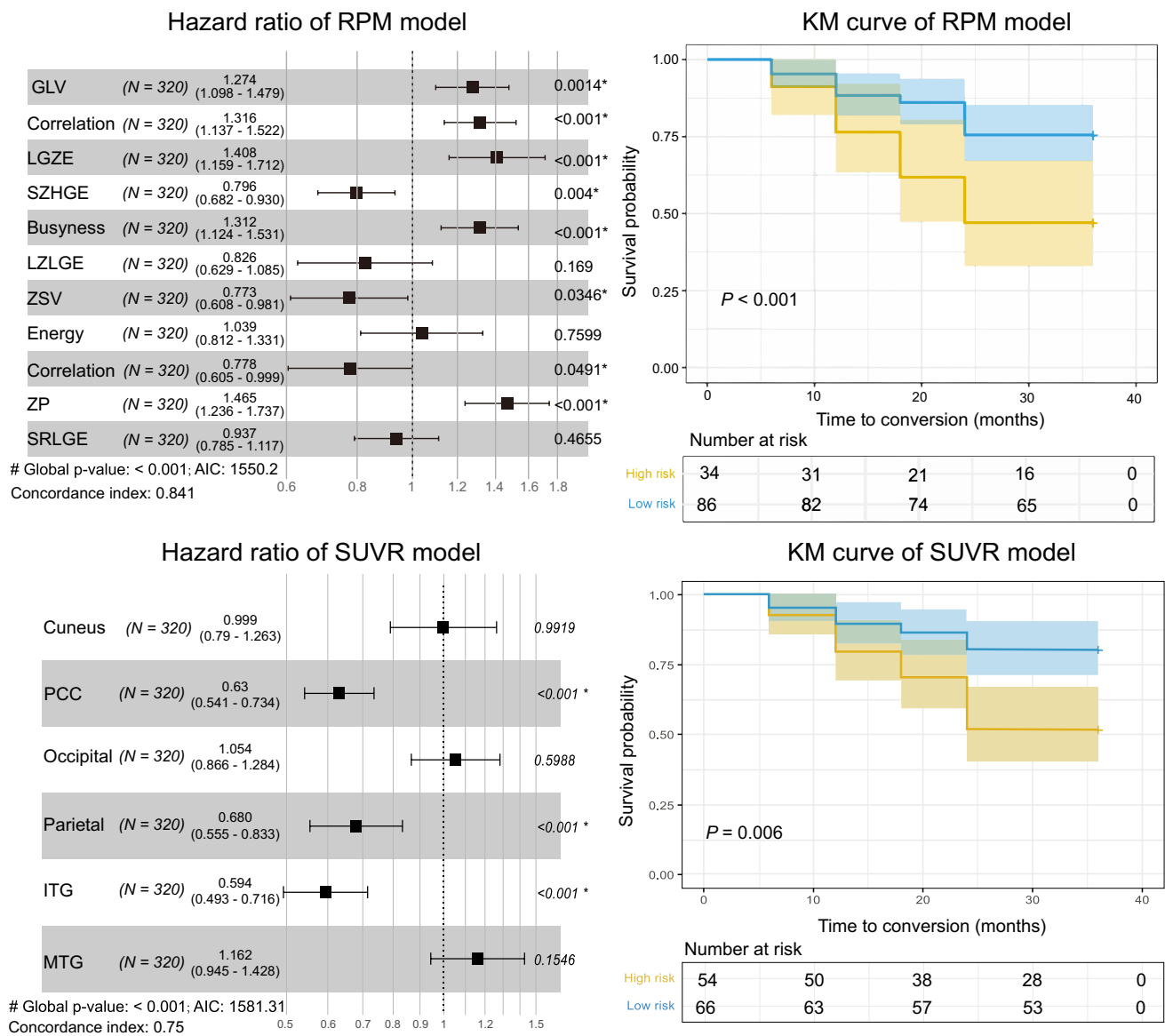


Fig. 2 Hazard ratios for different predictors and Kaplan–Meier survival curves. RPM model was constructed by 11 identified features, and SUVR model was constructed by 6 composite SUVR values

(Table S1). PCC, posterior cingulate cortex; ITG, inferior temporal gyri; MTG, middle temporal pole gyri

validated our methodology using independent ADNI data, and explored the correlation between optimal biomarkers and clinical information from local hospitals. Furthermore, the stratification effects of the predictors found in the study and the routine SUVR model were compared.

As a result, 34,400 quantitative features were extracted in 80 cortical regions for each modality of each subject. In this study, three Cox models were constructed based on the source of the features, and the performance of the RPM model was superior to that of the clinical and SUVR models. This may be related to the low sensitivity and higher subjectivity of the neuropsychological scales and the incomplete characteristics of the SUVR quantification [37]. On the

external test dataset (cohort II) in our study, the performance of the RPM model was also better than that of other models. These results further demonstrated that the methodology of this study is stable and reliable, thereby proving the great potential of quantitative features from PET images to predict MCI conversion.

In this study, we considered all cortical regions as ROIs and extracted quantitative features from them. Surprisingly, our study found that most of the selected conserved features were in areas consistent with previous studies, such as the hippocampus and parahippocampal gyrus in the temporal cortex, the precuneus and supramarginal gyrus in the parietal cortex, and the medial and paracingulate gyri in the frontal region.

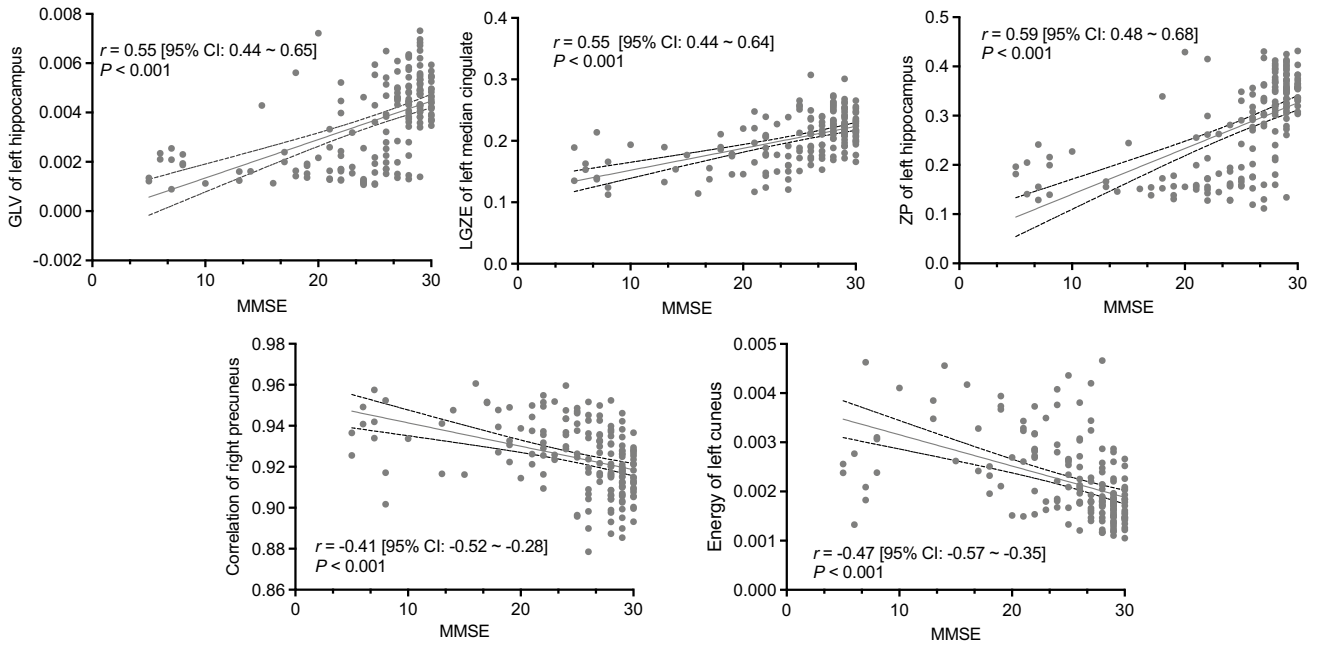


Fig. 3 The relationships between 5 identified radiomic features and neuropsychological assessments (MMSE scores). By saving the 100 bootstrapping derived r values, we obtained the 95% confidence interval (95% CI) and tested whether the r distribution deviated from zero

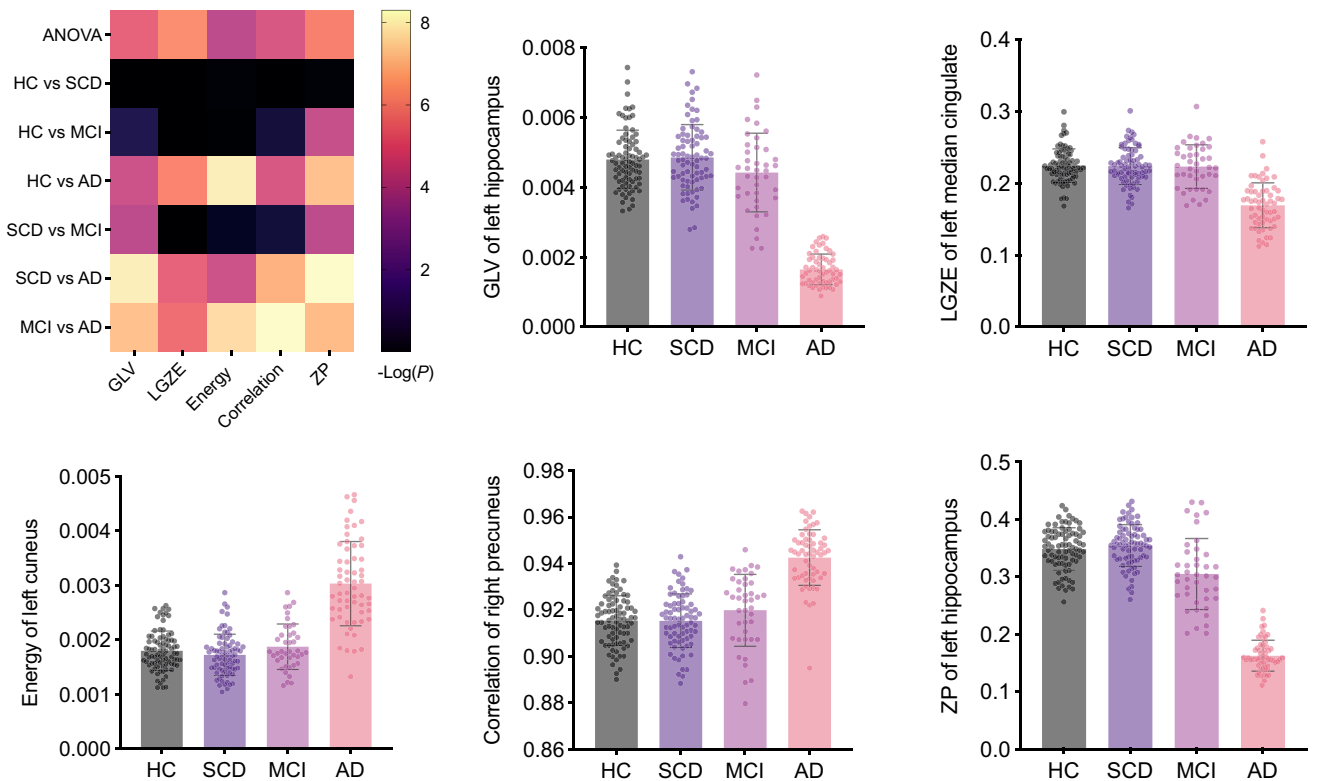


Fig. 4 Group differences of a subset of radiomic features at different cognitive stages. The P values were derived using ANOVA test and Dunnett's multiple comparison test

On the one hand, the medial temporal areas, precuneus, and cingulate gyrus are all brain regions of early AD-related pathological protein ($A\beta$ and hyperphosphorylated tau) deposition [4], and they are also regions with early atrophy, thickness reduction, or metabolism reduction [38–40]. On the other hand, atrophy or decreased metabolism of these regions is a robust biomarker for predicting MCI conversion. Based on the conserved texture features extracted from these regions, the constructed model had a better prediction efficiency than the SUVR model or clinical model. In addition, our study evaluated the changes in these crucial image markers at different cognitive stages in cross sections. Most features were significantly different among the HC, MCI, and AD groups. Conceptually, the GLV measures the variance of gray-level values in the zones with a greater value, indicating larger differences between the gray-level values and more heterogeneity of image texture [41]. From our perspective, these features may contain unique information about changes at the microscopic level that can occur before changes at the macroscopic level, which is in consistent with the ideas of previous studies [26]. In conclusion, our study confirmed that metabolic features from AD pathologically susceptible regions were more effective at predicting MCI conversion, and the metabolic abnormalities in these areas could be better represented by high dimensional radiomic features. Moreover, the results also provided strong evidence for using radiomic features to track the progress of high-risk individuals, which is important for clinical purposes.

Further correlation analyses suggested that the levels of features including GLV, LGZE, and ZP, were significantly and positively correlated with the MMSE scores, and other features including the correlation and energy showed a negative correlation. The results were consistent with their performance on the Alzheimer's continuum, specifically, the expression of positive (negative) correlation features in dementia subjects was significantly reduced (increased), suggesting their predictive roles in cognition [26].

We draw attention to some limitations of this study. First, the limited medical center was a barrier to the reproducibility of our RPM model. Further studies should assess its potential within larger and more heterogeneous external test groups. Second, this study lacked in-depth evaluation of the pathological mechanism, such as the pathological basis of crucial imaging markers, which could be further explored by combining genetic information and tau pathology in subsequent studies. Third, due to the lack of longitudinal data, the longitudinal changes in crucial bioimaging markers could not be explored.

Conclusions

In this study, we designed an approach for radiomics-based predictive modelling analysis on PET images. Our results demonstrated that the combination of radiomic

features extracted in the whole brain from PET images can more accurately predict MCI conversion, has good stability and reliability, and can be used for disease stratification management. Moreover, the results also provided strong evidence for using radiomic features to predict the risk in MCI patients to convert to AD, which is important for clinical purposes. These preliminary tests demonstrated the potential of the RPM method as a clinical auxiliary tool to help MCI conversion prediction.

Supplementary Information The online version contains supplementary material available at <https://doi.org/10.1007/s00259-022-05687-y>.

Acknowledgements Private sector contributions are facilitated by the Foundation for the National Institutes of Health (www.fnih.org). The grantee organization is the Northern California Institute for Research and Education, and the study is coordinated by the Alzheimer's Disease Cooperative Study at the University of California, San Diego, CA, USA. ADNI data are disseminated by the Laboratory for Neuro Imaging at the University of Southern California, CA, USA.

Funding This article was supported by grants from the National Natural Science Foundation of China (61603236 and 81830059, 81971641, 81671239, and 81361120393), Shanghai Municipal Science and Technology Major Project (No. 2017SHZDZX01, 2018SHZDZX03), and 111 Project (D20031). Data collection and sharing for this project were funded by the Alzheimers Disease Neuroimaging Initiative (ADNI; National Institutes of Health Grant U01 AG024904) and DODADNI (Department of Defense, award number W81XWH-12-2-0012). ADNI is funded by the National Institute of Aging and the National Institute of Biomedical Imaging and Bioengineering and through generous contributions from the following: AbbVie, Alzheimer's Association; Alzheimer's Drug Discovery Foundation; Araclon Biotech; BioClinica, Inc.; Biogen; Bristol-Myers Squibb Company; CereSpir, Inc.; Eisai, Inc.; Elan Pharmaceuticals, Inc.; Eli Lilly and Company; EuroImmun; F.Hoffmann-La Roche Ltd. and its affiliated company Genentech, Inc.; Fujirebio; GE Healthcare; IXICO Ltd.; Janssen Alzheimer Immunotherapy Research & Development, LLC.; Johnson & Johnson Pharmaceutical Research & Development LLC.; Lumosity; Lundbeck; Merck & Co., Inc.; Meso Scale Diagnostics, LLC.; NeuroRx Research; Neurotrack Technologies; Novartis Pharmaceuticals Corporation; Pfizer, Inc.; Piramal Imaging; Servier; Takeda Pharmaceutical Company; and Transition Therapeutics. The Canadian Institutes of Health Research is providing funds to support ADNI clinical sites in Canada.

Data availability The data that support the findings of this study are available from ADNI database and the corresponding author.

Declarations

Consent to participate Not applicable.

Research involving human participants and/or animals The research involved human participants. Data used in this project was approved by institutional review boards of ADNI, Huashan Hospital, and Xuanwu Hospital, and written informed consent was obtained from all participants or authorized representatives.

Conflict of interest The authors declare no competing interests.

References

- 2020 Alzheimer's disease facts and figures. *Alzheimers Dement*. 2020. <https://doi.org/10.1002/alz.12068>.
- Scheltens P, Blennow K, Breteler MM, de Strooper B, Frisoni GB, Salloway S, et al. Alzheimer's disease. *Lancet*. 2016;388(10043):505–17. [https://doi.org/10.1016/S0140-6736\(15\)01124-1](https://doi.org/10.1016/S0140-6736(15)01124-1).
- Jack CR Jr, Wiste HJ, Weigand SD, Therneau TM, Lowe VJ, Knopman DS, et al. Defining imaging biomarker cut points for brain aging and Alzheimer's disease. *Alzheimers Dement*. 2017;13(3):205–16. <https://doi.org/10.1016/j.jalz.2016.08.005>.
- Long JM, Holtzman DM. Alzheimer disease: an update on pathobiology and treatment strategies. *Cell*. 2019;179(2):312–39. <https://doi.org/10.1016/j.cell.2019.09.001>.
- Jack CR Jr, Bennett DA, Blennow K, Carrillo MC, Dunn B, Haeberlein SB, et al. NIA-AA Research framework: toward a biological definition of Alzheimer's disease. *Alzheimers Dement*. 2018;14(4):535–62. <https://doi.org/10.1016/j.jalz.2018.02.018>.
- Mitchell AJ, Shiri-Feshki M. Rate of progression of mild cognitive impairment to dementia—meta-analysis of 41 robust inception cohort studies. *Acta Psychiatr Scand*. 2009;119(4):252–65. <https://doi.org/10.1111/j.1600-0447.2008.01326.x>.
- Farias ST, Mungas D, Reed BR, Harvey D, DeCarli C. Progression of mild cognitive impairment to dementia in clinic- vs community-based cohorts. *Arch Neurol*. 2009;66(9):1151–7. <https://doi.org/10.1001/archneurol.2009.106>.
- Schneider JA, Arvanitakis Z, Leurgans SE, Bennett DA. The neuropathology of probable Alzheimer disease and mild cognitive impairment. *Ann Neurol*. 2009;66(2):200–8.
- Petersen RC, Roberts RO, Knopman DS, Boeve BF, Geda YE, Ivnik RJ, et al. Mild cognitive impairment ten years later. *Arch Neurol-Chicago*. 2009;66(12):1447–55.
- Dubois B, Hampel H, Feldman HH, Scheltens P, Aisen P, Andrieu S, et al. Preclinical Alzheimer's disease: definition, natural history, and diagnostic criteria. *Alzheimers Dement*. 2016;12(3):292–323. <https://doi.org/10.1016/j.jalz.2016.02.002>.
- Farrell ME, Jiang S, Schultz AP, Properzi MJ, Price JC, Becker JA, et al. Defining the lowest threshold for amyloid-PET to predict future cognitive decline and amyloid accumulation. *Neurology*. 2021;96(4):e619–31. <https://doi.org/10.1212/wnl.000000000011214>.
- Salvadó G, Molinuevo JL, Brugulat-Serrat A, Falcon C, Grau-Rivera O, Suárez-Calvet M, et al. Centiloid cut-off values for optimal agreement between PET and CSF core AD biomarkers. *Alzheimer's Res Ther*. 2019;11(1):27. <https://doi.org/10.1186/s13195-019-0478-z>.
- Fakhry-Darian D, Patel NH, Khan S, Barwick T, Svensson W, Khan S, et al. Optimisation and usefulness of quantitative analysis of (18)F-florbetapir PET. *Br J Radiol*. 2019;92(1101):20181020. <https://doi.org/10.1259/bjr.20181020>.
- Kreisl WC, Kim M-J, Coughlin JM, Henter ID, Owen DR, Innis RB. PET imaging of neuroinflammation in neurological disorders. *The Lancet Neurology*. 2020;19(11):940–50. [https://doi.org/10.1016/s1474-4422\(20\)30346-x](https://doi.org/10.1016/s1474-4422(20)30346-x).
- Blazhenets G, Ma Y, Sörensen A, Rucker G, Schiller F, Eidelberg D, et al. Principal components analysis of brain metabolism predicts development of Alzheimer dementia. *J Nucl Med*. 2019;60(6):837–43. <https://doi.org/10.2967/jnumed.118.219097>.
- Shen T, Jiang J, Lu J, Wang M, Zuo C, Yu Z, et al. Predicting Alzheimer disease from mild cognitive impairment with a deep belief network based on 18F-FDG-PET images. *Mol Imaging*. 2019;18:1536012119877285. <https://doi.org/10.1177/1536012119877285>.
- Wang M, Jiang J, Yan Z, Alberts I, Ge J, Zhang H, et al. Individual brain metabolic connectome indicator based on Kullback-Leibler Divergence Similarity Estimation predicts progression from mild cognitive impairment to Alzheimer's dementia. *Eur J Nucl Med Mol Imaging*. 2020;47(12):2753–64. <https://doi.org/10.1007/s00259-020-04814-x>.
- Landau SM, Harvey D, Madison CM, Koeppe RA, Reiman EM, Foster NL, et al. Associations between cognitive, functional, and FDG-PET measures of decline in AD and MCI. *Neurobiol Aging*. 2011;32(7):1207–18. <https://doi.org/10.1016/j.neurobiolaging.2009.07.002>.
- Cabral C, Morgado PM, Costa DC, Silveira M, Initi AsDN. Predicting conversion from MCI to AD with FDG-PET brain images at different prodromal stages. *Comput Biol Med*. 2015;58:101–9. <https://doi.org/10.1016/j.combiomed.2015.01.003>.
- Pagani M, Giuliani A, Öberg J, De Carli F, Morbelli S, Girtler N, et al. Progressive disintegration of brain networking from normal aging to Alzheimer disease: analysis of independent components of (18)F-FDG PET data. *J Nucl Med*. 2017;58(7):1132–9. <https://doi.org/10.2967/jnumed.116.184309>.
- Rizzo S, Botta F, Raimondi S, Origgi D, Fanciullo C, Morganti AG, et al. Radiomics: the facts and the challenges of image analysis. *Eur Radiol Exp*. 2018;2(1):1–8.
- Lambin P, Leijenaar RT, Deist TM, Peerlings J, De Jong EE, Van Timmeren J, et al. Radiomics: the bridge between medical imaging and personalized medicine. *Nat Rev Clin Oncol*. 2017;14(12):749.
- Hu X, Sun X, Hu F, Liu F, Ruan W, Wu T, et al. Multivariate radiomics models based on (18)F-FDG hybrid PET/MRI for distinguishing between Parkinson's disease and multiple system atrophy. *Eur J Nucl Med Mol Imaging*. 2021;48(11):3469–81. <https://doi.org/10.1007/s00259-021-05325-z>.
- Wu Y, Jiang JH, Chen L, Lu JY, Ge JJ, Liu FT, et al. Use of radiomic features and support vector machine to distinguish Parkinson's disease cases from normal controls. *Ann Transl Med*. 2019;7(23):773. <https://doi.org/10.21037/atm.2019.11.26>.
- Zhou H, Jiang J, Lu J, Wang M, Zhang H, Zuo C. Dual-model radiomic biomarkers predict development of mild cognitive impairment progression to Alzheimer's disease. *Front Neurosci*. 2018;12:1045. <https://doi.org/10.3389/fnins.2018.01045>.
- Li TR, Wu Y, Jiang JJ, Lin H, Han CL, Jiang JH, et al. Radiomics analysis of magnetic resonance imaging facilitates the identification of preclinical Alzheimer's disease: an exploratory study. *Front Cell Dev Biol*. 2020;8: 605734. <https://doi.org/10.3389/fcell.2020.605734>.
- Li X, Wang X, Su L, Hu X, Han Y. Sino Longitudinal Study on Cognitive Decline (SILCODE): protocol for a Chinese longitudinal observational study to develop risk prediction models of conversion to mild cognitive impairment in individuals with subjective cognitive decline. *BMJ Open*. 2019;9(7): e028188. <https://doi.org/10.1136/bmjopen-2018-028188>.
- McKhann GM, Knopman DS, Chertkow H, Hyman BT, Jack CR Jr, Kawas CH, et al. The diagnosis of dementia due to Alzheimer's disease: recommendations from the National Institute on Aging-Alzheimer's Association workgroups on diagnostic guidelines for Alzheimer's disease. *Alzheimers Dement*. 2011;7(3):263–9. <https://doi.org/10.1016/j.jalz.2011.03.005>.
- Jessen F, Amariglio RE, Van Boxtel M, Breteler M, Ceccaldi M, Chételat G, et al. A conceptual framework for research on subjective cognitive decline in preclinical Alzheimer's disease. *Alzheimers Dement*. 2014;10(6):844–52.
- Bondi MW, Edmonds EC, Jak AJ, Clark LR, Delano-Wood L, McDonald CR, et al. Neuropsychological criteria for mild cognitive impairment improves diagnostic precision, biomarker associations, and progression rates. *J Alzheimer's Dis: JAD*. 2014;42(1):275–89. <https://doi.org/10.3233/jad-140276>.

31. Landau SM, Mintun MA, Joshi AD, Koeppe RA, Petersen RC, Aisen PS, et al. Amyloid deposition, hypometabolism, and longitudinal cognitive decline. *Ann Neurol*. 2012;72(4):578–86. <https://doi.org/10.1002/ana.23650>.
32. Ge J, Wang M, Lin W, Wu P, Guan Y, Zhang H, et al. Metabolic network as an objective biomarker in monitoring deep brain stimulation for Parkinson's disease: a longitudinal study. *EJNMMI Res*. 2020;10(1):131. <https://doi.org/10.1186/s13550-020-00722-1>.
33. Woo CW, Chang LJ, Lindquist MA, Wager TD. Building better biomarkers: brain models in translational neuroimaging. *Nat Neurosci*. 2017;20(3):365–77. <https://doi.org/10.1038/nn.4478>.
34. Simon N, Friedman J, Hastie T, Tibshirani R. Regularization paths for Cox's proportional hazards model via coordinate descent. *J Stat Softw*. 2011;39(5):1.
35. Friedman J, Hastie T, Tibshirani R. Regularization paths for generalized linear models via coordinate descent. *J Stat Softw*. 2010;33(1):1.
36. Therneau TM, Grambsch PM. *Modeling survival data: extending the Cox model*. Springer Science & Business Media; 2013.
37. Huang K, Lin Y, Yang L, Wang Y, Cai S, Pang L, et al. A multipredictor model to predict the conversion of mild cognitive impairment to Alzheimer's disease by using a predictive nomogram. *Neuropsychopharmacology*. 2020;45(2):358–66. <https://doi.org/10.1038/s41386-019-0551-0>.
38. Kato T, Inui Y, Nakamura A, Ito K. Brain fluorodeoxyglucose (FDG) PET in dementia. *Ageing Res Rev*. 2016;30:73–84. <https://doi.org/10.1016/j.arr.2016.02.003>.
39. Pini L, Pievani M, Bocchetta M, Altomare D, Bosco P, Cavado E, et al. Brain atrophy in Alzheimer's disease and aging. *Ageing Res Rev*. 2016;30:25–48. <https://doi.org/10.1016/j.arr.2016.01.002>.
40. Risacher SL, Saykin AJ. Neuroimaging in aging and neurologic diseases. *Handb Clin Neurol*. 2019;167:191–227. <https://doi.org/10.1016/b978-0-12-804766-8.00012-1>.
41. Wang X, Song G, Jiang H, Zheng L, Pang P, Xu J. Can texture analysis based on single unenhanced CT accurately predict the WHO/ISUP grading of localized clear cell renal cell carcinoma? *Abdom Radiol (NY)*. 2021;46(9):4289–300. <https://doi.org/10.1007/s00261-021-03090-z>.

Publisher's note Springer Nature remains neutral with regard to jurisdictional claims in published maps and institutional affiliations.